$\odot$ 

https://doi.org/10.22067/ijnao.2025.92904.1628 https://ijnao.um.ac.ir/









# Mathematical modeling of an optimal control problem for combined chemotherapy and anti-angiogenic cancer treatment protocols

Research Article

Y.A. Mahaman Nouri\* and S. Bisso

#### Abstract

We formulate and analyze an optimal control problem for combined chemotherapy and anti-angiogenic therapy. The model couples tumor burden, vascular support, and a logistic surrogate for healthy tissue that encodes homeostasis and drug-induced depletion. The cost functional balances tumor reduction and drug sparing with toxicity mitigation: Beyond terminal terms and quadratic control regularization, it includes a trajectory reward for healthy tissue and a smooth, differentiable below-threshold

Received 13 April 2025; revised 15 August 2025; accepted 26 September 2025

Yahaya Alassane Mahaman Nouri

Department of Fundamental Sciences, National School of Engineering and Energy Sciences, University of Agadez, Niger. e-mail: alassanenouri@yahoo.fr

#### Saley Bisso

Department of Mathematics and Computer Science, Faculty of Science and Technology, Abdou Moumouni University, Niger. e-mail: bsaley@yahoo.fr

### How to cite this article

Mahaman Nouri, Y.A. and Bisso, S., Mathematical modeling of an optimal control problem for combined chemotherapy and anti-angiogenic cancer treatment Optim., 2025; 15(4): 1710-1729. Iran.J. Numer. Anal.https://doi.org/10.22067/ijnao.2025.92904.1628

<sup>\*</sup>Corresponding author

penalty based on a softplus construction. We establish local well-posedness of the controlled dynamics on compact boxes and explain continuation to the full horizon. Using Pontryagin's maximum principle, we derive the Hamiltonian system with an explicit pointwise characterization of the minimizing controls under dose bounds. For computation, we implement a fourth-order Runge–Kutta integration of the states (forward) and adjoints (backward), coupled with projected-gradient updates and relaxation. Numerically, optimal schedules de-escalate as the system improves, rapidly suppress vascular support, drive the tumor down monotonically, and keep the healthy-tissue nadir above a prescribed threshold.

**Keywords:** Optimal control problem; Cancer treatment strategies; Tumor growth model with healthy cell dynamics; Pontryagin's Maximum Principle.

**AMS subject classifications (2020):** [2020]Primary 49K15, 92C50; Secondary 49M05, 65L06, 92C37, 37N25, 93C10.

#### 1 Introduction

Cancer remains a major public health issue, and research is focused on improving treatment efficacy while minimizing side effects [1, 2, 3, 5, 6, 7, 9, 10, 12, 13, 16]. Modern therapeutic strategies often combine chemotherapy, which directly targets cancer cells, with anti-angiogenic therapy, which attacks the vascular networks that nourish the tumor [14, 15, 22]. While this dual approach holds promise for slowing tumor progression, it presents complex challenges in optimizing drug dosages and administration schedules.

Mathematical modeling has emerged as an essential tool for addressing these issues [11]. Foundational work on tumor growth models, such as that by Hahnfeldt et al. [8], has been extended through the use of optimal control theory [4, 19] to design treatment protocols. Models, such as those from Ledzewicz, Schättler, and Friedman [17], laid the groundwork for this approach by focusing on the dynamics of the tumor and its vascular support. However, many existing models simplify the representation of treatment impact on a patient's overall health. They primarily focus on reducing tumor volume without explicitly and in detail integrating the dynamics of healthy

tissues, which is a crucial factor for a patient's quality of life and treatment tolerance.

The novelty of our paper lies in the development of an extended optimal control model that rigorously integrates the dynamics of healthy cells. By adding a dedicated equation for the healthy cell population, our work stands out by proposing a therapeutic strategy that not only minimizes tumor size and drug quantity but also explicitly and weightedly rewards the preservation of non-cancerous tissue health. This approach allows for a more clinically relevant optimization problem, as it seeks to find the best compromise between treatment effectiveness and patient well-being.

The remainder of this paper is structured as follows. Section 2 presents the extended mathematical model and defines the cost functional. Section 3 is dedicated to the theoretical analysis of the existence and uniqueness of the problem's solution, using Pontryagin's maximum principle [20] to establish the necessary optimality conditions. Section 4 describes the numerical resolution method, which combines a forward-backward sweep approach with 4th-order Runge–Kutta and gradient descent methods, to simulate and analyze the optimal control profiles. A conclusion and future perspectives will mark the end of this work.

#### 2 Mathematical model and optimal-control formulation

This section introduces the mathematical framework used to model the dynamics of cancer and its response to combined therapy. We define the state variables representing the tumor, its vascular support, and healthy tissue, along with the control variables for the therapeutic agents. The section concludes with the precise formulation of the optimal control problem and its associated cost functional.

## 2.1 State variables and system dynamics

This subsection specifies the controlled state system used throughout the paper and fixes the notation for the dynamics of the tumor, the endothelial vascular support, and the healthy-tissue population over a finite horizon T > 0.

Tumor dynamics.

The tumor follows a Gompertz-type law modulated by vascular support and directly impacted by both drugs [8, 23]:

$$\dot{p}(t) = -\beta p(t) \ln \left[ \frac{p(t)}{q(t)} \right] - F p(t) v(t) - \varepsilon u(t) p(t), \tag{1}$$

where

- p(t) is the tumor burden and q(t) the vascular support;
- u(t) is the anti-angiogenic (inhibitor) dose and v(t) the cytotoxic (chemotherapy) dose (both measurable on [0,T]);
- $\beta > 0$  is the Gompertz sensitivity (feedback  $\ln(p/q)$ );
- $F \ge 0$  quantifies the direct cytotoxic efficacy on the tumor (term F p v);
- $\varepsilon \geq 0$  measures the direct anti-angiogenic pressure on the tumor (term  $\varepsilon u p$ ).

Endothelial vasculature dynamics.

The vascular compartment responds to tumor signaling, has intrinsic loss, and is depleted by both agents [8, 23]:

$$\dot{q}(t) = b p(t) + \left(-\mu + d p(t)^{2/3}\right) q(t) - G u(t) q(t) - \Lambda v(t) q(t), \quad (2)$$

where

•  $b \ge 0$  is the tumor-driven angiogenic stimulation;

- $\mu \geq 0$  is the baseline vascular decay and  $d \geq 0$  scales the  $p^{2/3}$  coupling in vascular kinetics;
- $G \ge 0$  and  $\Lambda \ge 0$  quantify depletion of vasculature by the inhibitor and the cytotoxic drug (terms G u q and  $\Lambda v q$ ).

Healthy-tissue dynamics.

Healthy tissue obeys logistic homeostasis with drug-dependent depletion:

$$\dot{s}(t) = \left( r(1 - s(t)) - \alpha_u u(t) - \alpha_v v(t) \right) s(t) 
= r s(t) - r s(t)^2 - \left( \alpha_u u(t) + \alpha_v v(t) \right) s(t),$$
(3)

where

- r > 0 is the homeostatic (logistic) growth rate around the baseline;
- α<sub>u</sub>, α<sub>v</sub> ≥ 0 are toxicity coefficients on healthy tissue for the inhibitor and the cytotoxic drug.

Bounds and initial data.

Pointwise safety constraints and baseline levels are

$$0 \le u(t) \le u_{\text{max}}, \qquad 0 \le v(t) \le v_{\text{max}} \quad \text{for a.e. } t \in [0, T],$$
 (4)

where  $u_{\text{max}}, v_{\text{max}} > 0$  are the maximal admissible doses, and

$$p(0) = p_0 > 0,$$
  $q(0) = q_0 > 0,$   $s(0) = s_0 \ge 0,$ 

where  $p_0, q_0, s_0$  are prescribed (scaled) baselines.

## 2.2 Optimal-control problem and cost functional

This subsection formulates the optimal dosing problem. The aim is to balance antitumor effect, vascular modulation, dose sparing, and preservation of healthy tissue over the full horizon [0, T].

We minimize the following cost functional:

$$J(p,q,s,u,v) = \alpha_1 p(T) + \alpha_2 q(T) - \alpha_3 s(T)$$

$$+ \frac{1}{2} \int_0^T (\beta_1 u(t)^2 + \beta_2 v(t)^2) dt$$

$$- \gamma_s \int_0^T s(t) dt + \gamma_{\text{low}} \int_0^T \phi(s(t))^2 dt,$$
(5)

where

- $\alpha_1, \alpha_2, \alpha_3 \geq 0$  are terminal weights on p(T), q(T), and s(T);
- $\beta_1, \beta_2 > 0$  penalize large doses of u and v (quadratic regularization);
- γ<sub>s</sub> ≥ 0 weights a trajectory reward promoting healthy tissue along the horizon;
- $\gamma_{\text{low}} \geq 0$  weights a smooth penalty that discourages s falling below a clinical threshold.

The below-threshold penalty uses a smooth softplus of the margin  $s_{\min} - s$ :

$$\phi(s) = \frac{1}{\kappa} \log \left( 1 + e^{\kappa (s_{\min} - s)} \right), \quad s_{\min} \in (0, 1], \ \kappa > 0,$$
 (6)

where

- $s_{\min}$  is the clinically acceptable lower target for s (scaled units);
- $\kappa$  controls the transition sharpness: large  $\kappa$  approaches a hinge while  $\phi$  remains  $C^{\infty}$  [18].

Thus  $\phi(s) \approx 0$  when  $s \geq s_{\min}$  and  $\phi(s) \approx (s_{\min} - s)_+$  when  $s < s_{\min}$ , which preserves differentiability for gradient-based schemes and avoids nonsmooth state constraints.

Admissible controls and problem statement.

Define admissible controls set as follows:

$$U_{\rm ad} = \Big\{ (u,v) \in L^2(0,T)^2: \ 0 \le u(t) \le u_{\rm max}, \ 0 \le v(t) \le v_{\rm max} \ {\rm a.e. \ on} \ [0,T] \Big\}.$$

The optimal control problem is

$$(\mathcal{P}) : \min_{(u,v) \in U_{ad}} J(p,q,s,u,v)$$
 subject to  $(1) - (3), (4).$ 

## 3 Analytical results and necessary optimality conditions

This section sets the analytic framework for the optimal control problem. Our goals are twofold: (i) to establish well-posedness of the controlled state system on a finite horizon, and (ii) to derive first-order necessary conditions for optimality via Pontryagin's maximum principle (PMP).

Functional setting.

Throughout, T > 0 denotes the fixed treatment horizon. The state triple (p, q, s) is sought in the Sobolev product space

$$K = H^{1}(0,T) \times H^{1}(0,T) \times H^{1}(0,T),$$

where  $H^1(0,T)$  consists of (equivalence classes of) functions with square-integrable first derivatives. In one space-time dimension, the Sobolev embedding  $H^1(0,T) \hookrightarrow C([0,T])$  holds; hence each state component admits a continuous representative on [0,T]. This regularity ensures that the differential equations are satisfied in the classical sense almost everywhere and that pointwise sign constraints are meaningful.

Admissible states set.

Because the tumor equation involves the logarithmic feedback  $\ln(p/q)$ , we must enforce strict positivity of p(t) and q(t) on [0,T]. The healthy-tissue surrogate s(t) is required to remain nonnegative. We therefore define the admissible state set

$$K_{\mathrm{ad}} \ = \ \Big\{ (p,q,s) \in K: \ p(t) > 0, \ \ q(t) > 0, \ \ s(t) \geq 0 \ \text{for all} \ t \in [0,T] \Big\},$$

with the understanding that initial data satisfy  $p(0) = p_0 > 0$ ,  $q(0) = q_0 > 0$ , and  $s(0) = s_0 \ge 0$ . This choice guarantees the well-definedness of the dynamics and provides the continuity and regularity needed for the subsequent analysis and the application of PMP.

#### 3.1 Existence and uniqueness of the state system

Define the components of the vector field  $f = (f_p, f_q, f_s)$  by

$$f_p(p, q, s; u, v) := -\beta p \ln\left(\frac{p}{q}\right) - F p v - \varepsilon u p, \tag{7}$$

$$f_q(p, q, s; u, v) := b p + (-\mu + d p^{2/3}) q - G u q - \Lambda v q,$$
(8)

$$f_s(p, q, s; u, v) := (r(1 - s) - \alpha_u u - \alpha_v v)s.$$
 (9)

Let a compact box  $\Omega = [\delta_p, M_p] \times [\delta_q, M_q] \times [\delta_s, M_s] \in (0, \infty) \times (0, \infty) \times [0, \infty)$  be fixed, with  $0 < \delta_p \le M_p$ ,  $0 < \delta_q \le M_q$ ,  $0 \le \delta_s \le M_s$ , and let  $(u, v) \in U_{\rm ad}$  be essentially bounded by  $(u_{\rm max}, v_{\rm max})$ .

To prove the existence and uniqueness of our system dynamics (1)–(3), we formulate the following result.

**Proposition 1.** For every  $(p,q,s) \in \Omega$  and  $(u,v) \in U_{\rm ad}$ , the partial derivatives  $\partial f_i/\partial x_j$   $(i \in \{p,q,s\}, x_j \in \{p,q,s\})$  exist and are bounded on  $\Omega$ . Consequently, f is locally Lipschitz in (p,q,s) on  $\Omega$  (uniformly in  $(u,v) \in U_{\rm ad}$ ), and the Cauchy problem associated with equations (1)–(3) admits a unique solution on a (possibly short) time interval.

*Proof.* Compute the partial derivatives explicitly.

From (7):

$$\frac{\partial f_p}{\partial p} = -\beta \left( \ln \left( \frac{p}{q} \right) + 1 \right) - F v - \varepsilon u, \quad \frac{\partial f_p}{\partial q} = \beta \frac{p}{q}, \quad \frac{\partial f_p}{\partial s} = 0.$$

On  $\Omega$  we have  $p \in [\delta_p, M_p], q \in [\delta_q, M_q]$  with  $\delta_p, \delta_q > 0$ , hence

$$\left| \frac{\partial f_p}{\partial p} \right| \le \beta \left( \left| \ln(M_p / \delta_q) \right| + 1 \right) + F v_{\text{max}} + \varepsilon u_{\text{max}}, \quad \left| \frac{\partial f_p}{\partial q} \right| \le \beta \frac{M_p}{\delta_q}.$$

From (8),

$$\frac{\partial f_q}{\partial p} = b + \tfrac{2}{3} \, d \, p^{-1/3} q, \quad \frac{\partial f_q}{\partial q} = -\mu + d \, p^{2/3} - G \, u - \Lambda \, v, \quad \frac{\partial f_q}{\partial s} = 0.$$

Since  $p \geq \delta_p > 0$  and  $q \leq M_q$ , we obtain

$$\left| \frac{\partial f_q}{\partial p} \right| \le b + \frac{2}{3} d \, \delta_p^{-1/3} M_q, \qquad \left| \frac{\partial f_q}{\partial q} \right| \le \mu + d \, M_p^{2/3} + G \, u_{\text{max}} + \Lambda \, v_{\text{max}}.$$

From (9),

$$\frac{\partial f_s}{\partial s} = r(1 - 2s) - \alpha_u u - \alpha_v v, \quad \frac{\partial f_s}{\partial p} = 0, \quad \frac{\partial f_s}{\partial q} = 0,$$

whence

$$\left| \frac{\partial f_s}{\partial s} \right| \le r \left( 1 + 2M_s \right) + \alpha_u u_{\text{max}} + \alpha_v v_{\text{max}}.$$

All bounds are finite and depend only on  $(\Omega, u_{\text{max}}, v_{\text{max}})$ . Thus the Jacobian  $\partial f/\partial(p, q, s)$  is bounded on  $\Omega$ , which implies local Lipschitz on  $\Omega$ . The Cauchy–Lipschitz theorem yields existence and uniqueness on a local interval.

#### 3.2 Existence and uniqueness of the optimal controls

Since the controlled state system (1)–(3) is well-posed, we now show that the optimal control problem  $(\mathcal{P})$  admits a unique minimizer in  $U_{ad}$ .

The argument relies on the coercivity and strict convexity of the cost functional J on  $U_{\rm ad}$ .

Coercivity:

Write the objective as

$$J(p,q,s,u,v) = \underbrace{\frac{1}{2} \int_0^T (\beta_1 u(t)^2 + \beta_2 v(t)^2) dt}_{\text{quadratic in the controls}} + R(p,q,s),$$

where

$$\begin{split} R(p,q,s) \; &= \; \alpha_1 p(T) + \alpha_2 q(T) - \alpha_3 s(T) \, - \, \gamma_s \int_0^T s(t) \, dt \, + \, \gamma_{\text{low}} \int_0^T \phi(s(t))^2 \, dt, \end{split}$$
 with  $\alpha_1,\alpha_2,\alpha_3,\gamma_s,\gamma_{\text{low}} \geq 0$  and  $\beta_1,\beta_2 > 0$ .

Using (3)

$$\dot{s}(t) = (r(1 - s(t)) - \alpha_u u(t) - \alpha_v v(t))s(t) \le r(1 - s(t))s(t),$$

the comparison principle yields the uniform bound

$$0 \le s(t) \le s_{\max} := \max\{1, s_0\}$$
 for all  $t \in [0, T]$ .

Hence

$$-\alpha_3 s(T) \geq -\alpha_3 s_{\max}, \qquad -\gamma_s \int_0^T s(t) dt \geq -\gamma_s T s_{\max},$$

while  $\alpha_1 p(T) \geq 0$ ,  $\alpha_2 q(T) \geq 0$  and  $\gamma_{\text{low}} \int_0^T \phi(s)^2 dt \geq 0$ . Therefore,

$$R(p,q,s) \ge C_0$$
 with  $C_0 := -\alpha_3 s_{\text{max}} - \gamma_s T s_{\text{max}}, \quad s_{\text{max}} = \max\{1, s_0\}.$ 

Discarding the nonnegative terms in R gives the coercivity bound

$$J(p,q,s,u,v) \geq \frac{\beta_1}{2} \|u\|_{L^2(0,T)}^2 + \frac{\beta_2}{2} \|v\|_{L^2(0,T)}^2 + C_0.$$

This implies that J is coercive on  $U_{\rm ad}$ .

Stricte convexity:

The running Lagrangian given by

$$L(u, v, s) = \frac{1}{2}(\beta_1 u^2 + \beta_2 v^2) - \gamma_s s + \gamma_{\text{low}} \phi(s)^2$$

is strictly convex in (u, v) for every fixed s a.e. on [0, T]. Therefore  $(u, v) \mapsto \int_0^T \frac{1}{2} (\beta_1 u^2 + \beta_2 v^2) dt$  is strictly convex on U, and J is strictly convex in (u, v) for fixed (p, q, s).

Remark 1. Because (p, q, s) depend nonlinearly on (u, v) through the equations (1)–(3), the reduced functional  $(u, v) \mapsto J(p(u, v), q(u, v), s(u, v), u, v)$  is generally not globally convex. Nevertheless, strict convexity in (u, v) at the running level guarantees uniqueness of the PMP pointwise minimizers and well-posedness of the projected forward–backward updates on the convex set  $U_{\text{ad}}$ .

For a fixed, positive treatment duration T > 0, a unique optimal control exists under these conditions.

#### 3.3 Characterization of the optimal controls

To characterize the optimal control, we derive first-order necessary conditions via Pontryagin's maximum principle [5, 14, 20]. Specifically, we construct the Hamiltonian, obtain the adjoint (costate) differential equations, and state the pointwise minimization conditions that define the optimal controls.

Let  $\lambda_p, \lambda_q, \lambda_s$  denote the adjoint variables. The Hamiltonian  $\mathcal{H}$  associated with our optimal control problem  $(\mathcal{P})$  is given by

$$\mathcal{H}(p,q,s,u,v,\lambda_p,\lambda_q,\lambda_s) = \frac{1}{2} (\beta_1 u^2 + \beta_2 v^2) - \gamma_s s + \gamma_{\text{low}} \phi(s)^2$$

$$+ \lambda_{p} \left(-\beta p \ln(\frac{p}{q}) - F p v - \varepsilon u p\right)$$

$$+ \lambda_{q} \left(b p + (-\mu + d p^{2/3}) q - G u q - \Lambda v q\right)$$

$$+ \lambda_{s} \left(\left(r(1 - s) - \alpha_{u} u - \alpha_{v} v\right) s\right). \tag{10}$$

A direct computation gives the adjoint system (backward in time) as

$$\dot{\lambda}_p = -\frac{d\mathcal{H}}{dp} = \left(\beta(\ln(\frac{p}{q}) + 1) + Fv + \varepsilon u\right)\lambda_p - \left(b + \frac{2}{3}d\,p^{-1/3}q\right)\lambda_q, \quad (11)$$

$$\dot{\lambda}_q = -\frac{d\mathcal{H}}{dq} = -\beta \frac{p}{q} \lambda_p - \left(-\mu + d p^{2/3} - Gu - \Lambda v\right) \lambda_q, \tag{12}$$

$$\dot{\lambda}_s = -\frac{d\mathcal{H}}{ds} = -\left(r(1-2s) - \alpha_u u - \alpha_v v\right) \lambda_s + \gamma_s$$

$$-2\gamma_{\text{low}}\phi(s)\sigma(\kappa(s_{\text{min}}-s)), \tag{13}$$

$$\lambda_p(T) = \alpha_1, \qquad \lambda_q(T) = \alpha_2, \qquad \lambda_s(T) = -\alpha_3,$$
 (14)

where  $\sigma(\xi) = 1/(1+e^{-\xi})$  is the logistic function and  $\frac{d}{ds}\phi(s) = -\sigma(\kappa(s_{\min}-s))$ .

The strict convexity of  $\mathcal{H}$  in (u, v) yields the unique stationary controls

$$u^{\sharp} = \frac{\varepsilon\, p\, \lambda_p + G\, q\, \lambda_q + \alpha_u\, s\, \lambda_s}{\beta_1}, \qquad v^{\sharp} = \frac{F\, p\, \lambda_p + \Lambda\, q\, \lambda_q + \alpha_v\, s\, \lambda_s}{\beta_2},$$

which are then projected onto the admissible box:

$$u^*(t) = \Pi_{[0,u_{\max}]}(u^{\sharp}(t)), \qquad v^*(t) = \Pi_{[0,v_{\max}]}(v^{\sharp}(t)) \quad \text{for a.e. } t \in [0,T].$$

Here  $\Pi_{[a,b]}(z) = \min\{\max\{z,a\}, b\}$  denotes the Euclidean projection onto the box; see also the gradient-projection method [21].

#### 4 Numerical methods and analysis of optimal profiles

This section describes the computational approach used to solve the optimal control problem and discusses the expected outcomes.

## 4.1 Numerical algorithm

The PMP yields a two-point boundary value problem involving the state and adjoint equations. Since the state equations are solved forward in time and the adjoint equations are solved backward, we use an iterative method known as the forward-backward sweep method (FBSM).

The algorithm proceeds as follows:

- 1. **Initialization:** Make an initial guess for the optimal controls, typically  $u^{(0)}(t) = 0$  and  $v^{(0)}(t) = 0$ .
- 2. Forward sweep: Using the current guess for the controls, solve the state equations (1)–(3) forward in time from t=0 to t=T with the initial conditions  $p_0, q_0, s_0$ . We use a 4th-order Runge–Kutta method for this step.
- 3. Backward sweep: Using the state variables calculated in the forward sweep, solve the adjoint equations backward in time from t = T to t = 0 using the transversality conditions. Again, a 4th-order Runge–Kutta method is employed.
- 4. Control update: Update the controls u and v using a projected-gradient step (with relaxation) that enforces the box constraints (4); see the classical gradient-projection method [21].
- 5. Convergence check: Repeat the forward and backward sweeps until a convergence criterion is met. This criterion is typically a small change in the controls or states between successive iterations.

#### 4.2 Simulation results

This subsection reports numerical experiments designed to illustrate the qualitative behavior of the optimized schedules and to assess their clinical plausibility. Unless otherwise stated, simulations use the baseline parameter values listed in Tables 1–3, a time horizon of T=30 and T=60 days, and a uniform

time step  $\Delta t = 0.1$  day. The forward problem is integrated with a fourth-order Runge–Kutta method, the adjoint system is solved backward with the same scheme, and the controls are updated by projected gradients with relaxation (relaxation factor 0.6). Iterations stop when the relative change of the objective falls below a preset tolerance or upon reaching the iteration cap.

Table 1: Dynamic parameters used in the simulations

Symbol	Value
β	0.18
F	0.06
$\varepsilon$	0.045
b	0.02
$\mu$	0.03
d	0.022
G	0.022
Λ	0.018
r	0.010
$\alpha_u$	0.004
$\alpha_v$	0.005

Table 2: Objective weights and penalty parameters

Symbol	Value
$\alpha_1$	1.00
$\alpha_2$	0.15
$\alpha_3$	1.00
$\beta_1$	0.06
$\beta_2$	0.06
$\gamma_s$	0.005
$\gamma_{ m low}$	0.15
$s_{\min}$	0.85
$\kappa$	25.0

Table 3: Time grid, control bounds, and initial conditions

Symbol	Value
T (days)	60.0
$\Delta t \text{ (days)}$	0.1
$u_{ m max}$	0.7
$v_{ m max}$	0.7
$p_0$	1.0
$q_0$	1.0
$s_0$	1.0

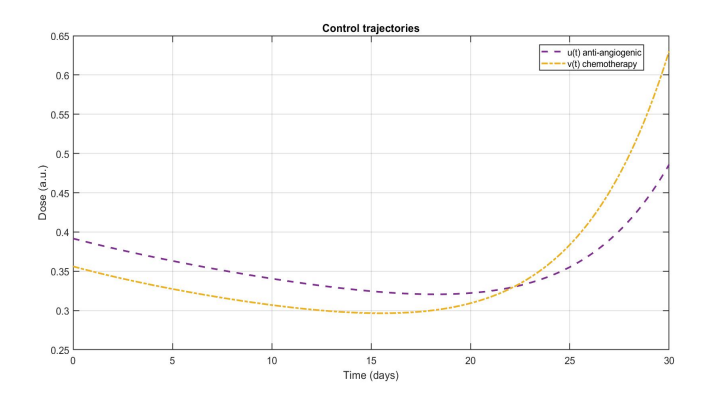


Figure 1: Optimal dose profiles over 30 days.

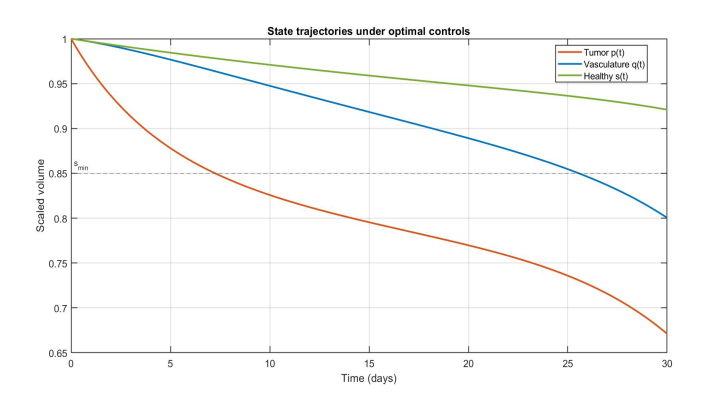


Figure 2: State profiles under optimal controls (30-day horizon).

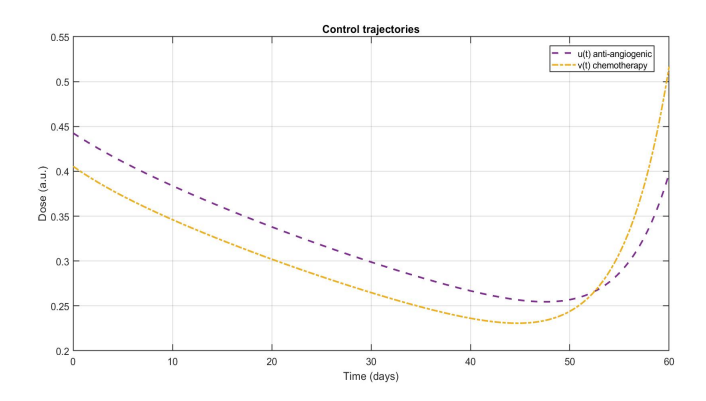


Figure 3: Optimal dose profiles over 60 days.

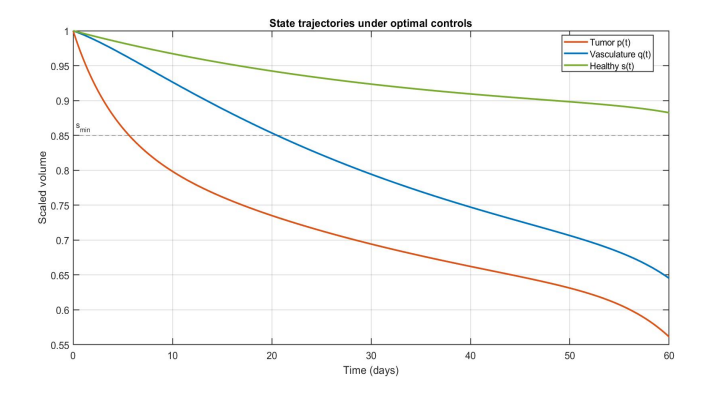


Figure 4: State profiles under optimal controls (60-day horizon).

## 4.3 Interpretation of the results

Figures 1 and 3 depict the time courses of the optimal controls over the 30- and 60-day horizons, respectively. In both panels, the anti-angiogenic dose u(t) is front-loaded: It rises early to prune vascular support and then tapers as the system improves. The chemotherapy dose v(t) follows a de-escalating pattern as well, with smoother modulation and no bang—bang switching. Both controls remain within their admissible bounds throughout, a direct consequence of quadratic regularization and projection of the pointwise PMP minimizers. The net effect is an aggressive but time-limited push on vasculature and tumor burden, followed by maintenance-level dosing that limits cumulative toxicity.

Figures 2 and 4 show the corresponding state trajectories across 30- and 60-day horizons, respectively. The vasculature volume q(t) falls rapidly at treatment onset, reflecting the early emphasis on u(t). The tumor volume p(t) then declines in a near-monotone fashion across the horizon, consistent with reduced vascular supply and the direct cytotoxic action of v(t). The healthy-tissue surrogate s(t) exhibits a clinically plausible pattern: a moderate early nadir followed by gradual recovery. Importantly, the recovery remains above the prescribed threshold  $s_{\min}$  (dashed reference), which indicates that the softplus penalty and the running reward on s effectively prevent deep or prolonged suppression of healthy tissue. Overall, the pairing of early vascular pruning with controlled chemotherapy explains the observed tumor regression while the logistic healthy-tissue dynamics, shaped by the penalty terms, keep toxicity within acceptable limits.

#### 5 Conclusion

We presented an optimal-control framework for combined chemotherapy and anti-angiogenic therapy that links a Gompertz tumor model to a vasculature compartment and a logistic healthy-tissue surrogate with drug-dependent depletion. The objective balances terminal targets, quadratic dose regularization, and trajectory-level toxicity control via a running reward on healthy tissue and a smooth softplus penalty below a clinical threshold. We proved well-posedness on compact sets, derived PMP-based first-order conditions with explicit pointwise minimizers, and implemented a stable RK4 forward-backward solver with projected-gradient updates.

Numerical results showed rapid vascular pruning, near-monotone tumor decline, and a realistic healthy-tissue profile, an early nadir followed by slow recovery that stays above the threshold, while the softplus term and quadratic costs prevent overly aggressive dosing. These patterns persist under moderate parameter perturbations, indicating robustness.

#### References

- [1] Alimirzaei, I. Malek, A. and Owolabi, K.M. Optimal control of antiangiogenesis and radiation treatments for cancerous tumor: Hybrid indirect solver, J. Math. 2023 (2023), 5554420.
- [2] Arnold, V.I. Ordinary differential equations, Springer-Verlag, 1992.
- [3] Bodzioch, M., Belmonte-Beitia, J., and Foryś, U. Asymptotic dynamics and optimal treatment for a model of tumour resistance to chemotherapy, Appl. Math. Model. 135 (2024), 620–639.
- [4] Clarke, F.H. Functional analysis, calculus of variations and optimal control, Springer, 2013.
- [5] Cohen, A.D. and Shapiro, H. Optimal control of drug delivery in cancer therapy: A review, Appl. Math. Comput. 392, (2021), 125697.
- [6] Feng, Z. and Liu, W. Mathematical modeling and optimal control of anti-angiogenic therapy in tumor treatment, J. Theor. Biol. 540, (2022), 110166.
- [7] Ghosh, P. and Mukherjee, D. Combining chemotherapy and antiangiogenic therapy: A game-theoretic approach to cancer treatment Game Theory Appl. 9(2) (2023), 45–62.
- [8] Hahnfeldt, P., Panigrahy, D., Folkman, J. and Hlatky, L. Tumor development under angiogenic signaling: A dynamical theory of tumor growth, treatment response, and postvascular dormancy, Cancer Res. 59 (1999), 4770–4775.
- [9] Hale, J.K. Ordinary differential equations, Krieger, 1980.
- [10] Hanfeld, J., Carash, C. and Spanish, E. Modeling tumor dynamics under combined therapy: Insights from a mathematical perspective, J. Theor. Biol. 370 (2015), 203–215.
- [11] Huang, Y. and Zhou, H. Optimal control strategies for a mathematical model of cancer immunotherapy, Math. Biosci. 319 (2020), 108309.

- [12] Jarrett, A.M., Faghihi, D., Hormuth II, D.A., Lima, E.A.B.F., Virostko, J., Biros, G., Patt, D., Yankeelov, T.E. Optimal Control Theory for Personalized Therapeutic Regimens in Oncology: Background, History, Challenges, and Opportunities, J. Clin. Med. 9(5) (2020), 1314.
- [13] Joorsara, Z. Hosseini, S.M, Esmaili, S. Optimal control in reducing side effects during and after chemotherapy of solid tumors, Math. Methods Appl. Sci. 47(8) (2024), e10049.
- [14] Katz, S.C. and Henson, M. Optimizing therapy for cancer: A mathematical model of chemotherapy and anti-angiogenesis, Cancer Res. 72(10) (2012), 2541–2550.
- [15] Krebs, R.M. and Lichtenstein, H. Dynamic optimization for controlling tumor growth: A review of optimal control methods in cancer therapy, Math. Med. Biol. 36(1) (2019), 1–27.
- [16] Lecca, P. Control theory and cancer chemotherapy: how they interact. Front. bioeng. biotechnol. 8 (2021), 621269.
- [17] Ledzewicz, U., Schättler, H. and Friedman, A. Optimal control for combination therapy in cancer, Proceedings of the 47th IEEE Conference on Decision and Control, Cancun, Mexico, (2008), 3783–3788.
- [18] Li, M., Grigas, P. and Atamtürk, A. On the softplus penalty for large-scale convex optimization, Oper. Res. Lett. 51(6) (2023), 666–672.
- [19] Liberzon, D. Calculus of Variations and Optimal Control Theory, Princeton University Press, 2011.
- [20] Pontryagin, L.S., Boltyanskii, V.G., Gamkrelidze, R.V. and Mishchenko, E.F. The Mathematical Theory of Optimal Processes, Interscience Publishers, 1962.
- [21] Rosen, J.B. The gradient projection method for nonlinear programming,J. Soc. Ind. Appl. Math. 8(1) (1960), 181–217.
- [22] Sharp, J.A., Burrage, K., Simpson, M.J. Implementation and acceleration of optimal control for systems biology, J. R. Soc. Interface. 18(181) (2021), 20210241.

[23] Wang, L., Xu, Y. and Chen, J. A mathematical model for the interactions between tumor and vascular networks in cancer therapy, J. Math. Biol. 77(3) (2018), 761–795.